Journal of Computation Physics and Earth Science
ISSN: 2776-2521 (online)
Volume 5, Number 2, February 2026, Page 162 - 172
https://journal.physan.org/index.php/jocpes/index

Meteorological Analysis of Strong Wind-Producing Clouds: A Case Study of Klaten, 18 November 2024

Febby Debora Abigael[1], Ahmad Hanif Al'aziz[2], Arya Zaki Ramadhan[3], Achmad Zakir[4], Aditya Mulya[5]
[1,2,3,4,5]Undergraduate Program in Meteorology (STMKG)

Article Info

Article history:

Received December 31, 2025
Revised March 5, 2026
Accepted March 5, 2026

Keywords:

Strong winds
Atmospheric dynamics
Cloud characteristics
Cumulonimbus cloud
Klaten

A B S T R A C T

Klaten Regency, Central Java, has frequently experienced extreme convective weather in the form of strong surface winds that have caused damage to residential areas and public facilities. This study analyzed a strong wind event that occurred on 18 November 2024 between 15:30 and 16:30 Local Time, which had significant impacts across several sub-districts in Klaten. The objective of this research was to evaluate the atmospheric dynamics and cloud characteristics responsible for the event. A descriptive–analytical approach was applied using secondary data, including the Dipole Mode Index, the Madden–Julian Oscillation Diagram, streamline map, and atmospheric stability indices to assess atmospheric dynamics. In addition, dual-polarization weather radar products were used to examine convective cloud structure, vertical development, wind convergence and divergence patterns, and indications of vortex formation. The results showed that the event was dominated by a rapidly developing Cumulonimbus cloud system, with maximum reflectivity values reaching approximately 69 dBZ and cloud-top heights of about 10 km. Low-level wind convergence and horizontal wind shear played a critical role in triggering deep convection. Atmospheric stability indices indicated sufficiently unstable conditions, although instability was not extreme. Doppler radar analysis revealed strong updraft–downdraft interactions, intense convergence–divergence patterns, and vortex formation during the mature stage of the storm.

Corresponden Author:

Febby Debora Abigael,
Undergraduate Program in Meteorology (STMKG)
Tangerang, Indonesia
Email: febbydeboraabigael@gmail.com

1. INTRODUCTION

Klaten Regency is a region in Central Java that is highly susceptible to severe convective weather, particularly strong winds [1]. This study is centered on a major event that occurred on 18 November 2024, from 15:30 to 16:30 Local Time (LT) (08:30 – 09:30 UTC), which caused extensive damage to residential buildings and public facilities across several sub-districts, including Gantiwarno, Kalikotes, Karanganom, and Klaten Utara [2]. The intensity and rapid development of this event necessitate a comprehensive evaluation of the atmospheric dynamics involved to better understand the storm's lifecycle and enhance local early warning systems. Severe convective weather is primarily driven by the rapid growth of Cumulonimbus clouds, where vertical air motion is a defining factor [3]. The interaction between extreme updrafts and powerful downdrafts is the fundamental mechanism behind damaging surface winds, such as downbursts [4]. Monitoring the vertical extension of reflectivity cores provides insight into the evolution of these updrafts, while Doppler radar technology is essential for identifying wind shear and vortex signatures that precede such destructive events. Specifically in Indonesia, low-level air mass convergence has been identified as a primary trigger for deep convection in tropical environments [5]. This research provides a novel contribution by integrating radar analysis to reconstruct the kinematic structure of a specific localized storm in Klaten. Consequently, the

objective of this research is to evaluate the atmospheric dynamics and radar signatures associated with the severe wind event in Klaten by examining the spatial and vertical growth patterns of convective cells, investigating the kinematic structures related to convergence and divergence zones, and assessing the potential for vortex formation and atmospheric instability during the storm's peak intensity. Unlike typical convective storms in Java, which are generally characterized by disorganized multi-cell systems or short-lived orographic rain, this event is uniquely distinguished by its rapid transition into a highly organized structure capable of producing extreme downbursts and localized vortex signatures. Such features are rarely observed in standard tropical convection over the region, making this case a critical benchmark for understanding small-scale yet high-impact wind phenomena in Central Java.

2. RESEARCH METHOD

This study uses descriptive–analytical and qualitative methods to describe and analyze phenomena in detail and to understand their patterns, relationships, and meanings [6]. The focus of the research is the Klaten Regency area, as shown in Figure 1, with data consisting of IOD, MJO, streamlines, atmospheric stability indices, and radar images related to strong winds, which are discussed in the following subpoints. To facilitate this study, observational data is derived from the Semarang Weather Radar located in Tambakaji, Ngaliyan (7.002° S, 110.350° E), which operates with a surveillance radius of 250 kilometers.

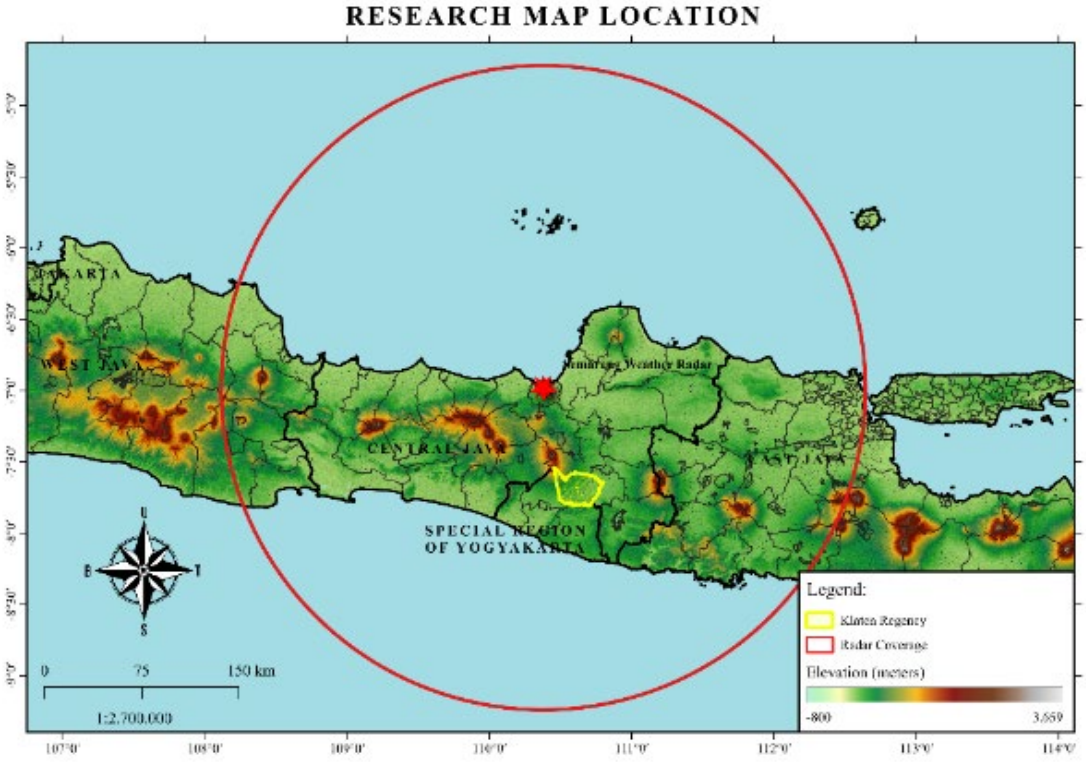

Fig. 1. Research Map Location

2.1. Data Collection Methods

This study uses secondary data for the analysis of IOD, MJO, streamlines, atmospheric stability, and cloud identification using radar imagery. The IOD data were accessed from NASA Jet Propulsion Laboratory (JPL) through https://sealevel.jpl.nasa.gov/overlay-iod/ in the form of the Dipole Mode Index (DMI), which represents the difference in sea surface temperature (SST) anomalies between the western and eastern Indian Ocean. This index was first introduced by Saji et al. (1999) [7] and is widely used in studies on regional climate variability in Indonesia.

Meanwhile, MJO data were obtained from the Australian Bureau of Meteorology (BoM) through the website https://www.bom.gov.au/climate/mjo/, including the RMM1 and RMM2 indices, amplitude, and daily MJO phases. The RMM index is used because it effectively represents the global position and strength of MJO convection, as developed by Wheeler and Hendon based on the Madden–Julian concept.

Streamline and atmospheric stability data were derived from the ERA5 Reanalysis Single Levels dataset provided by the Copernicus Climate Data Store (CDS) of the European Centre for Medium-Range Weather Forecasts (ECMWF) at a spatial resolution of 0.25° × 0.25°. ERA5 represents a fifth-generation global

atmospheric reanalysis that combines observational records with numerical weather prediction models to ensure a physically consistent depiction of atmospheric conditions [8]. Streamline patterns were examined using the zonal (u) and meridional (v) wind components [9], on 18 November 2024 from 08:00 to 10:00 UTC, whereas atmospheric stability was assessed using CAPE, CIN, KI, and TTI during 06:00–12:00 UTC on the same day.

The radar data used in this research were obtained from the Agency for Meteorology, Climatology, and Geophysics (BMKG) at the Ahmad Yani Meteorological Station, Semarang. The dataset was provided in .vol format and subsequently processed using Rainbow5 Software. The system utilized is a dual-polarization radar with a scanning interval of 10 minutes.

2.2. Data Processing Methods

IOD and MJO data processing only involves selecting the analysis time period, because the DMI values and MJO diagrams are obtained directly from the data source without recalculation. The u and v data for the streamline map, along with CAPE, CIN, KI, and TTI for atmospheric stability analysis, were obtained by selecting the study period and area and downloaded in NetCDF format, and furthermore, these data were processed using GrADS to produce streamline maps and atmospheric stability index graphs. Radar data were processed using Rainbow5 software via several specialized applications, with preprocessing performed using the 3D-RAVE application, which included Z-based attenuation correction, bright band correction, and clutter filtering to ensure data quality. Following this, the RainDART-TS application was used to generate various radar products, specifically Column Maximum (CMAX), Storm Structure Analysis (SSA), Vertical Cut (VCUT), Constant Altitude Plan Position Indicator (CAPPI/MCAPPI) Velocity, Tornado Vortex Detection (TVD), and the Severe Weather Indicator (SWI) [10], [11], where CMAX and SSA are used to identify the structure of Cumulonimbus cloud cells based on their reflectivity profiles [12], [13], while CAPPI Velocity is utilized to determine wind movement derived from particle displacement [14], [15], and finally, TVD and SWI are used to detect potential vortices, as well as wind divergence and convergence.

2.3. Data Analysis Method

IOD analysis focuses on the interpretation of DMI and its impact on Indonesia's climate. A positive IOD (DMI > +0.4) is characterized by a warmer western Indian Ocean and a cooler eastern Indian Ocean, resulting in reduced rainfall and increased drought potential. A neutral IOD ($-0.4 \leq$ DMI $\leq +0.4$) has a weak influence, with weather more affected by other factors such as the monsoon and MJO. A negative IOD (DMI < -0.4) is marked by a warmer eastern Indian Ocean, increasing water vapor and leading to generally higher rainfall. Each IOD phase is associated with tendencies for wet or dry seasons in Indonesia, following the framework of Saji et al. (1999) [7] and supported by subsequent studies, such as Adiwira et al. (2018) [16]. MJO analysis was carried out descriptively and focused on the phases that affect Indonesia, particularly the Maritime Continent, namely phases 4–5, where convection increases, cloud development occurs, and there is a high potential for rainfall. Conversely, when the MJO is in phases 2–3 (Indian Ocean) and 6–7 (Western Pacific), Indonesia tends to experience subsidence and low rainfall [17].

Streamline is a curve where at every point it is tangent to the instantaneous flow velocity vector and is used to depict atmospheric circulation patterns [18]. In this study, streamline analysis is applied to identify the dominant direction of lower-level winds, detect zones of convergence and divergence, and examine the influence of synoptic-scale circulation on regional wind patterns. High wind speeds are indicated by closely spaced streamlines due to strong pressure gradients, while convergent streamline patterns indicate potential upward motion and atmospheric instability.

Atmospheric stability analysis is conducted by reviewing CAPE, CIN, KI, and TTI according to their categories in Table 1. CAPE indicates the energy available for convection, CIN measures vertical air resistance [19], [20], KI represents thunderstorm potential, whereas TTI reflects conditions conducive to severe weather [21]. The higher the values of CAPE, KI, and TTI, the more unstable the atmosphere. Conversely, high CIN indicates a more stable atmosphere [19], [20], [21].

Table 1. Classification of Atmospheric Stability Index Values [22]

Level	CAPE (J/kg)	CIN (J/kg)	KI (°C)	TTI (°C)
Weak	<1000	<50	<29	<42
Moderate	1000–2500	51–199	29–37	42–46
Strong	>2500	>200	>37	>46

Radar imagery analysis begins by evaluating the spatial and temporal evolution of convective cells through the CMAX and Storm Structure Analysis SSA products [12], [13]. These tools are used to monitor the initiation of cloud growth and track the intensification of reflectivity cores as the storm system develops. To further examine the vertical characteristics of the storm, the Vertical Cut VCUT product is applied to generate

cross-sectional profiles [23]. This method allows for the determination of convective depth and the vertical extension of high-reflectivity cores, which are essential for identifying the mature stage of a convective system and assessing its potential to produce significant weather. The second phase of the analysis focuses on the kinematic properties and severe weather signatures using Doppler velocity and specialized detection algorithms. Radial velocity products, including CAPPI and MPPI, are analyzed at various altitudes to identify airflow patterns, specifically targeting areas of wind convergence and divergence that trigger vertical updrafts and downdrafts [24], [25]. Furthermore, the Tornado Vortex Detection (TVD) and Severe Weather Indicator (SWI) are utilized to locate vortex signatures and extreme wind shear within the storm cell. By correlating the interaction between vertical air movements and these automated detection signals, the analysis establishes the physical mechanisms responsible for severe weather phenomena occurring at the surface.

3. RESULTS AND DISCUSSION

The results and discussion in this case study include the analysis of IOD, MJO, streamlines, atmospheric stability, and radar image interpretation, which are described as follows:

3.1. Indian Ocean Dipole

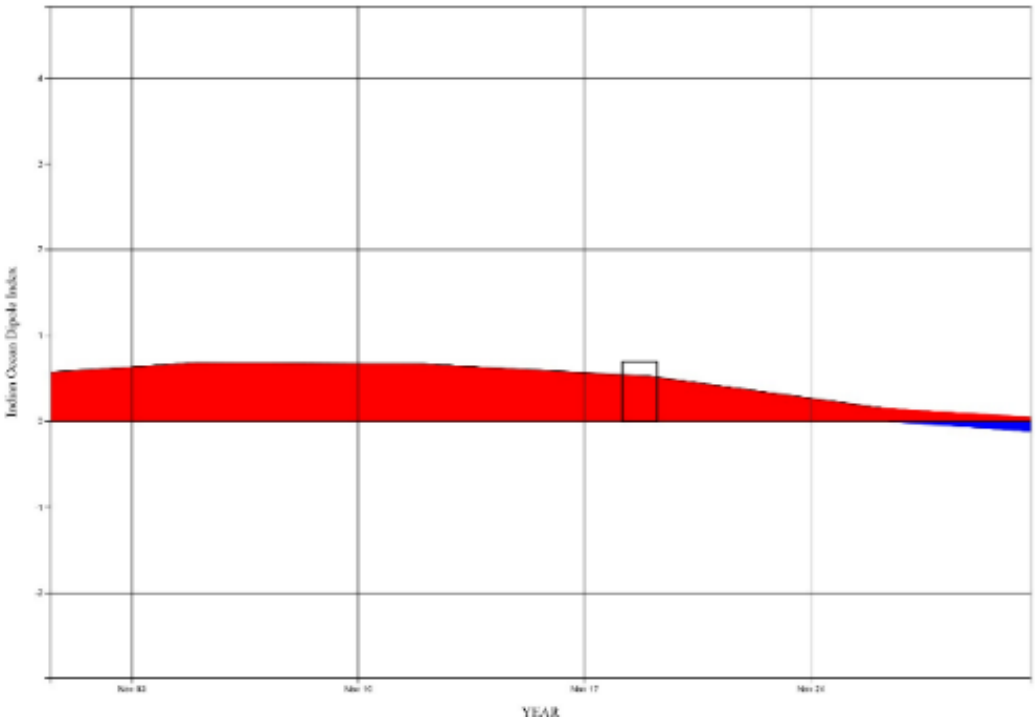

Fig. 2. DMI Chart

Based on Figure 2, during November 2024, the IOD remained in a positive phase during the first half of the month, with DMI values around +0.5 to +0.7, before gradually weakening towards neutral conditions. On 18 November 2024, the DMI was still positive at about +0.5, indicating a positive IOD event that was fading but still active. Positive IOD conditions are associated with cooler sea surface temperatures in the eastern Indian Ocean near Sumatra–Java and warmer conditions in the western basin, resulting in a strong zonal SST gradient [7]. Even during the weakening phase, residual SST and pressure gradients can persist and continue to influence atmospheric circulation. These conditions support abnormal east to southeast winds at the sea surface level in the eastern Indian Ocean, affecting the western regions of Sumatra and Java [16]. As a result, the weakening positive IOD on 18 November 2024, still contributed to the increase in surface wind conditions over Java.

3.2. Madden-Julian Oscillation

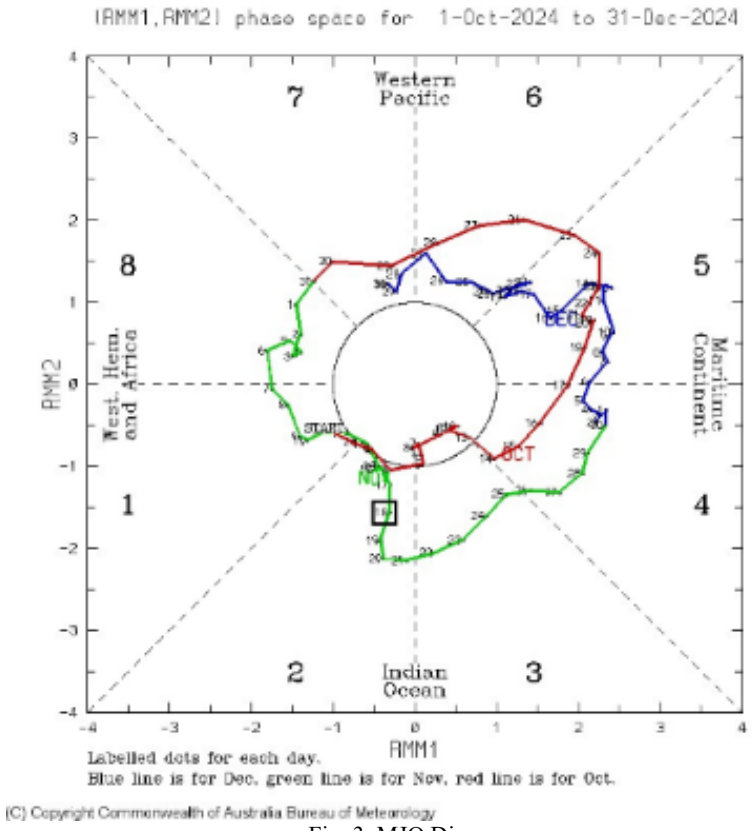

Fig. 3. MJO Diagram

As shown in Figure 3, the RMM phase-space diagram for October–December 2024 shows that on 18 November 2024 the Madden–Julian Oscillation (MJO) was active, as it lay outside the unit circle, and was positioned in Phase 2, approaching Phase 3. According to Madden and Julian (1972), an active MJO represents a large-scale coupled circulation–convection system capable of significantly modulating tropical atmospheric dynamics, indicating a dynamically important influence over Indonesia at that time [26]. Although MJO did not directly cause the storm, but it could enhance the background moisture and wind field, creating a preconditioned environment in which local mesoscale convergence could rapidly intensify [27]. Pattipeilohy and Asri (2019) showed that MJO Phases 2–3 are often linked to strengthened zonal wind anomalies due to enhanced convection over the eastern Indian Ocean [17]. Consequently, Java, located downstream of this convective region, is particularly sensitive to MJO-induced westerly wind intensification.

3.3. Streamline

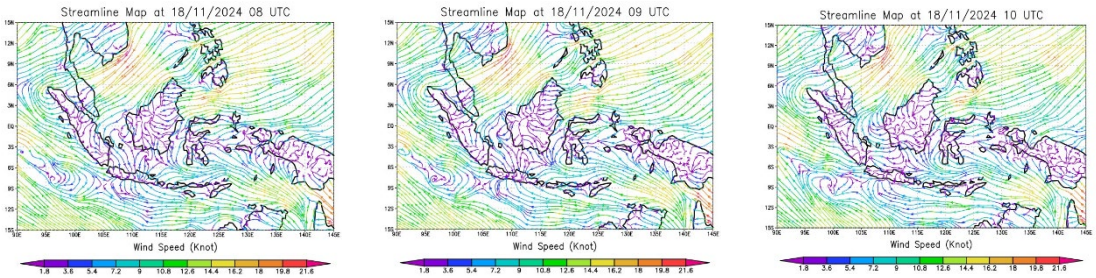

Fig. 4. Streamline Map on 18 November 2024

According to Figure 4, the low-level streamline evolution on 18 November 2024 between 08:00 and 10:00 UTC indicates that the strong wind event over Klaten and surrounding areas of Central Java was driven by regional-scale dynamics. At 08:00 UTC, a strengthening westerly to northwesterly monsoonal flow crossed Java, initiating low-level convergence over southern and central Java. By 09:00 UTC, the convergence intensified and became more organized, accompanied by increased wind curvature and horizontal shear, with

wind speeds reaching 10–14 knots. These conditions favored convective development and the generation of strong downdrafts and gust fronts, leading to damaging surface winds over Klaten. At 10:00 UTC, the convergence zone persisted but shifted slightly eastward, indicating a transition toward a weakening phase of the event.

3.4. Atmospheric Stability Index

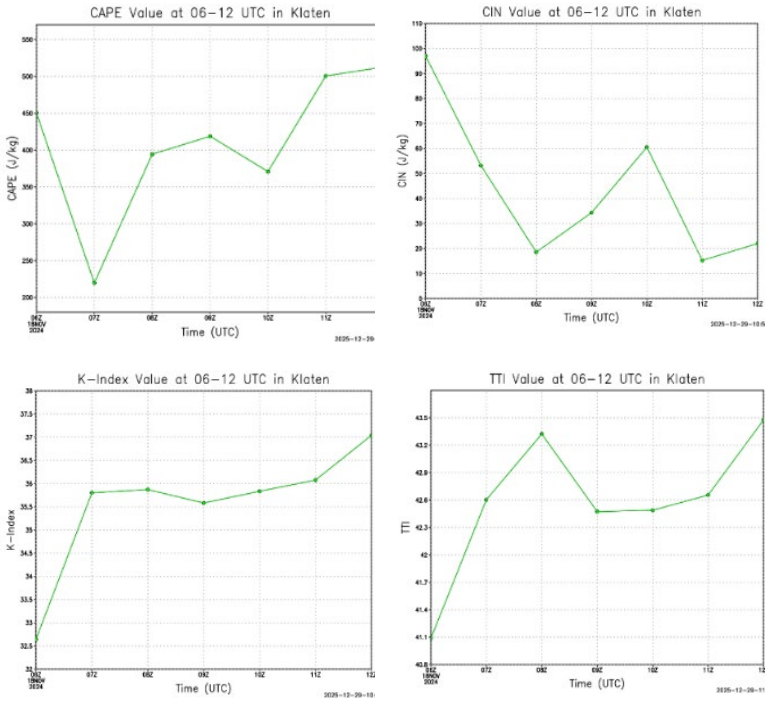

Fig. 5. Atmospheric Stability Index Chart

From Figure 5, it can be seen that the CAPE values are generally in the weak category [22], [28]. Nevertheless, there is a fairly significant increase at 08:00 UTC, and it continues to rise until 09:00 UTC with values around 390–420 J/kg, indicating an increase in convective activity, although the values are still relatively low. Meanwhile, CIN is in the moderate to weak range [22], with the weak category observed at 08:00–09:00 UTC and at 11:00 UTC. A significant decrease at 08:00 UTC, around 20 J/kg, indicates a relatively low inhibition to convection, allowing air to rise more easily into the upper layers of the atmosphere [19], [20]. Furthermore, KI is in the moderate category with values around 32.6–37°C [22], [28]. These values rise significantly towards 07:00–08:00 UTC and then experience slight fluctuations, indicating sufficient atmospheric instability to support the formation of local convection. Similarly, the TTI was in the weak to moderate range [22], [28], with moderate values recorded from 07:00 to 12:00 UTC. The most significant increase occurred at 08:00 UTC with a value of around 43.3°C, indicating that atmospheric instability reached a relatively high point during this period before slightly decreasing or remaining stable in the moderate range until 12:00 UTC. Like the KI, the TTI reflects sufficient atmospheric instability to support convective activity.

3.5. Weather Radar Imagery

Radar products used to analyze hail events include SSA overlay on CMAX, VCUT, MCAPPI (at an altitude of 3 km), TVD, and SWI.

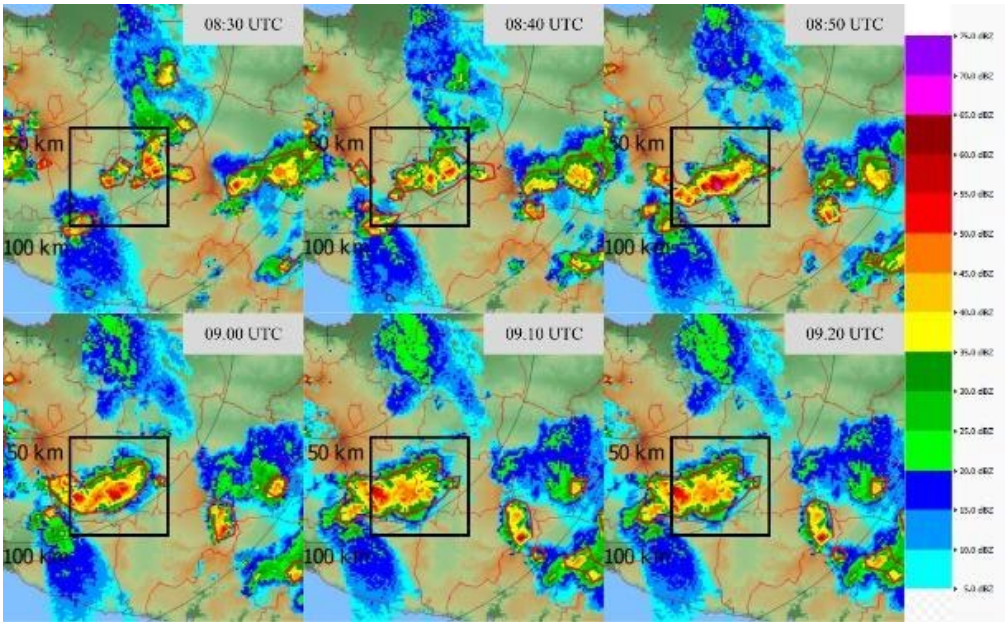

Fig. 6. SSA Overlay on CMAX Product

Table 2. Timeseries of Maximum Reflectivity

Maximum Reflectivity (dBZ)					
08:30	08:40	08:50	09:00	09:10	09:20
56.5	55.5	69	59	60.5	55.5

The CMAX product shows the growth of Cumulonimbus clouds starting to be seen at 08:30 UTC from the northeast of Klaten Regency. As delineated in Table 2, the storm's intensity experienced a rapid temporal evolution, highlighted by a surge in reflectivity from 55.5 dBZ at 08:40 UTC to its peak of 69 dBZ at 08:50 UTC while moving to the west. This significant growth in a fairly short time shows the presence of massive convective activity occurring at the location, indicating the potential for very strong cloud convergence and divergence. This intensification is further detailed by the Storm Structure Analysis (SSA), where red polygons delineate the active storm cells and the yellow polygons represent the cores of the Cumulonimbus cells. Initially, a single Cumulonimbus cell core was detected at 08:30 UTC, which subsequently developed into two distinct cores with very high reflectivity reaching peak intensity at 08:50 UTC. Reflectivity values remained high with a secondary maximum of 60.5 dBZ recorded at 09:10 UTC. Following this, the Cumulonimbus cells began to dissipate, characterized by the expansion of the cloud area and the fragmentation of the cores, as indicated by a notable decrease in reflectivity recorded between 09:00 and 09:20 UTC.

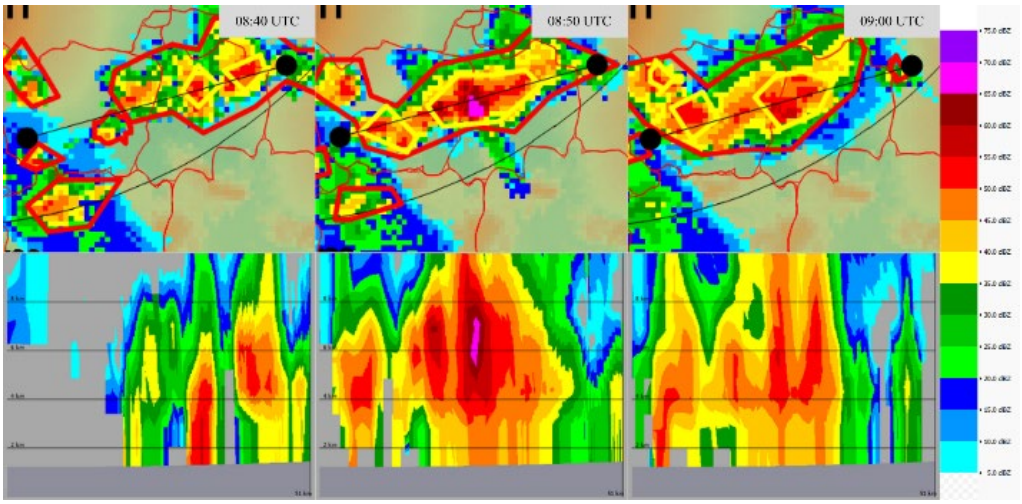

Fig. 7. SSA Overlay on CMAX Product and VCUT Product

The CMAX and VCUT products in Figure 7 illustrate the rapid development of Cumulonimbus clouds between 08:40 and 09:00 UTC. At 08:40 UTC, the clouds already showed significant vertical growth. By 08:50 UTC, the system reached its peak intensity, with reflectivity reaching a maximum of 69 dBZ (indicated by the

magenta core). The vertical cross-section at that time confirmed that the convective core towered up to about 10 km, indicating very strong convective activity. At 09:00 UTC, the cloud system remained intense and continued to develop, reflecting ongoing strong convergence and divergence within the atmosphere.

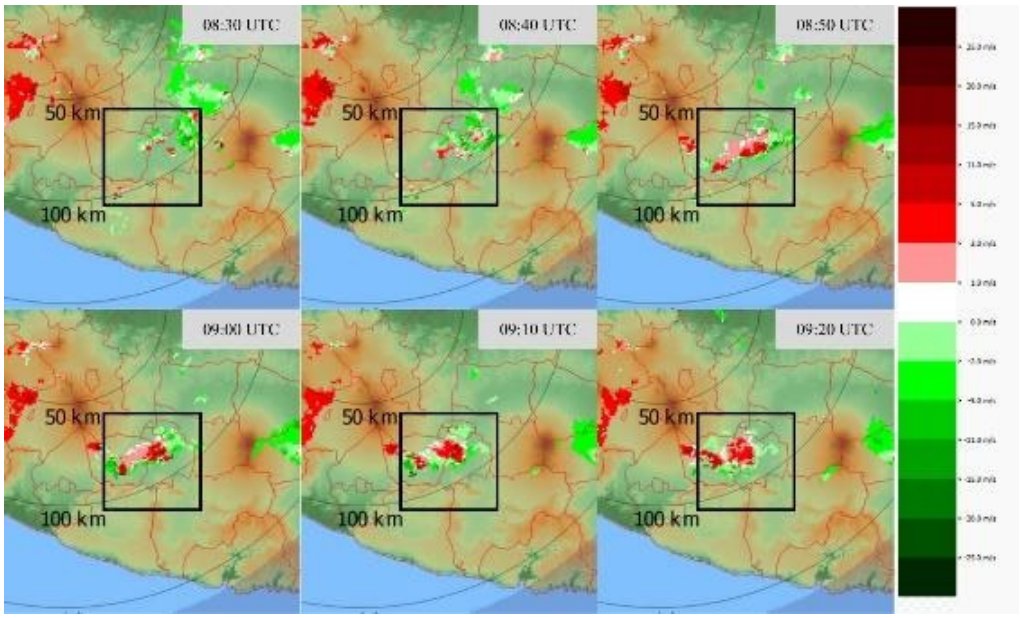

Fig. 8. MCAPPI Product

Weather conditions over Klaten Regency appeared to change drastically, as seen in Figure 8. Around 08:40 UTC, radar data showed a relatively uniform airflow moving toward the region. However, this situation did not last long. At an altitude of 3 kilometers above ground level, two air masses moving in opposite directions began to emerge. From one direction, the wind blew toward the radar (green), while from the other, the wind moved away from the radar (red). By 09:00 UTC, these two wind forces met directly over Klaten and its surroundings, creating a strong convergence zone. This collision of air masses forced the air at the meeting point to rise rapidly (updraft), triggering the formation of dense and towering Cumulonimbus clouds. It is within this storm cloud that the processes causing strong surface winds occurred. Cold air laden with raindrops inside the cloud became very heavy and eventually plunged downward at high speed.

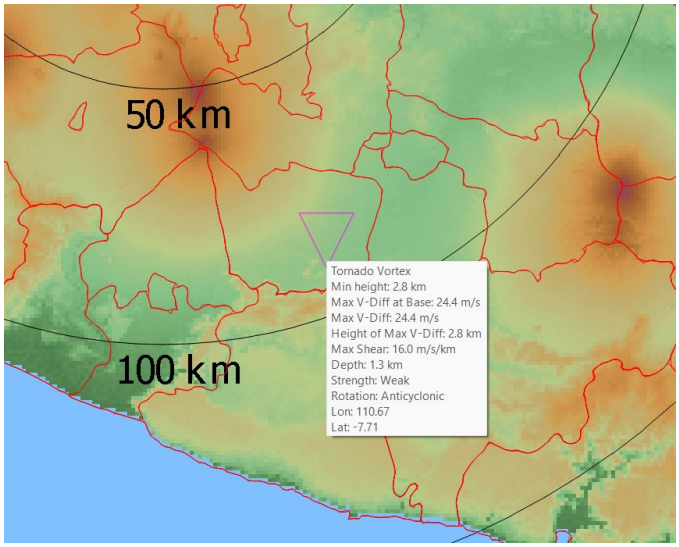

Fig. 9. TVD Product

Based on Figure 9, tornado vortex was detected at 09:10 UTC directly over the Klaten Regency area. This signifies the presence of opposing wind movements or shear, consistent with the interpretation of the previous wind velocity product.

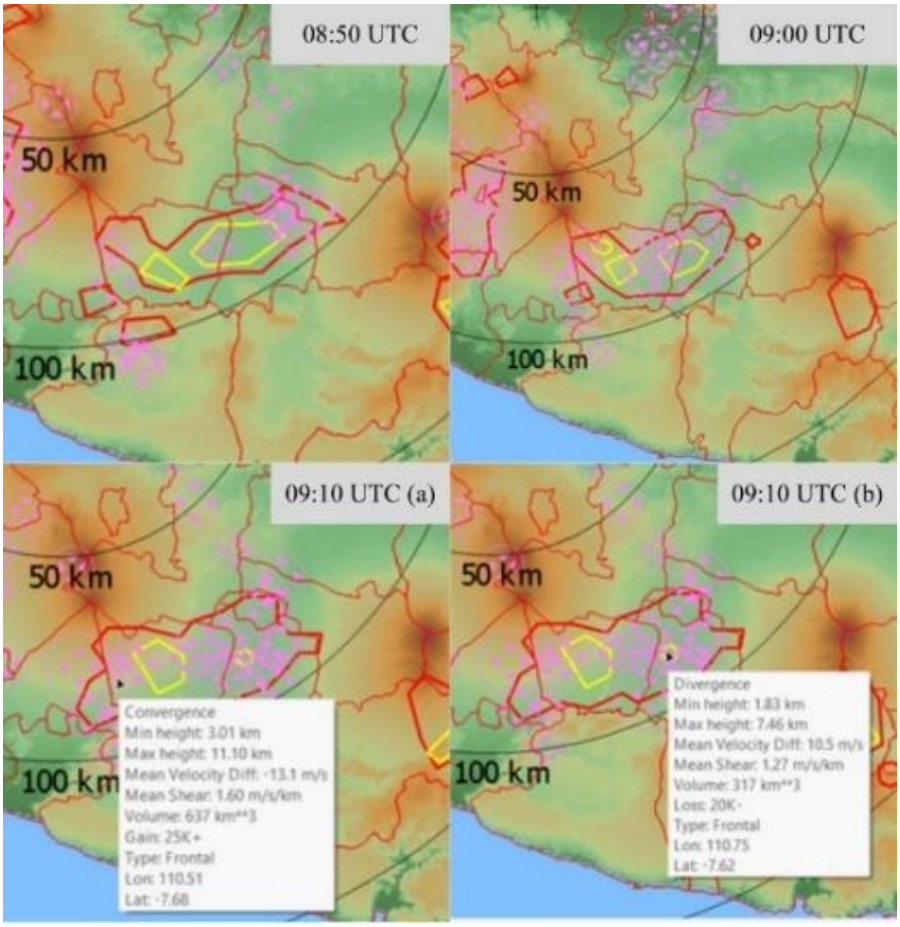

Fig. 10. SWI Product

According to Figure 10, it is observed that numerous convergence and divergence activities occurred within the same storm cell. Its rapid development is also visible, with the potential to cause significant weather at that time. The peak intensity of convective activity occurred at 09:10 UTC, when the radar simultaneously detected extreme convergence and divergence. The wind dynamics analysis was conducted by calculating the horizontal divergence ($\nabla \cdot V$) through the spatial derivatives of the horizontal wind components u and v as in Equation (1):

$$Div = \frac{\partial u}{\partial x} + \frac{\partial v}{\partial y} \quad (1)$$

Radar products such as the SWI is estimated based on the radial velocity difference ($\Delta V = V_{r,out} - V_{r,in}$) within a storm cell, where $\Delta V < 0$ represents convergence triggering updrafts, while $\Delta V > 0$ indicates divergence reflecting surface-bound downdrafts. Furthermore, the vortex intensity in TVD products was calculated based on the radial wind shear ($S = \Delta V_r / L$) to confirm the presence of a vortex [29]. The quantitative data indicates very strong convergence, extending vertically from an altitude of 3 km to the cloud top at 11.10 km, signaling a very powerful updraft. At the same time, strong divergence was detected, representing a downdraft from within the storm. The interaction between this extreme vertical updraft and the strong downdraft provides definitive evidence of a mature and intense storm cell, which served as the direct mechanism causing the damaging strong winds on the ground in Klaten.

4. CONCLUSION

The strong wind event in Klaten Regency on 18 November 2024, was triggered by a local mesoscale convective process, characterized by vertical growth of Cumulonimbus clouds, high reflectivity, significant convergence in the lower layers, and vortex formation, with downbursts as the main mechanism of the strong winds. The positive IOD phase (DMI ≈ +0.5) and active MJO (phase 2–3) over the eastern Indian Ocean enhanced the regional westerly flow and moisture transport toward Java. These large-scale drivers may not directly trigger the storm, but they helped the precondition of the atmosphere by supporting low-level convergence and a moderately unstable environment. Lower-layer streamlines indicated significant convergence and horizontal shear supporting the formation of local convection. Atmospheric stability indices

(CAPE, CIN, KI, TTI) showed the atmosphere was sufficiently unstable, facilitating cloud growth, albeit not extreme. Radar imagery shows the direct mechanism of strong winds occurring at the surface in Klaten, where CMAX recorded a maximum reflectivity of 69 dBZ at 08:50 UTC, SSA showed the core of the Cumulonimbus cell and active storm cells, VCUT indicated the convective core rising up to 10 km, MCAPPI indicated the meeting of two opposing air masses forming a strong convergence zone around 09:00 UTC, TVD detected a tornado vortex at 09:10 UTC, and SWI showed the presence of convergence and divergence resulting in damaging strong winds.

REFERENCE

[1] I. N. Saputro, F. A. Wakid, and S. S. Dewi, "Pembuatan Sistem Peringatan Dini Angin Puting Beliung di Desa Demakijo, Kecamatan Karangnongko, Kabupaten Klaten," BEMAS: Jurnal Bermasyarakat, vol. 4, no. 2, pp. 351–356, Mar. 2024, doi: 10.37373/bemas.v4i2.845.

[2] BNPB, "Data Informasi Bencana Indonesia (DIBI)," https://dibi.bnpb.go.id/. [Accessed: Dec. 26, 2025].

[3] B. HK. Tjasyono, Meteorologi Indonesia I: Karakteristik dan Sirkulasi Atmosfer, 4th ed., vol. 1. Badan Meteorologi, Klimatologi, dan Geofisika, 2012.

[4] R. R. Rogers and M. K. Yau, A Short Course in Cloud Physics, 3rd ed. Elsevier, 1989.

[5] D. Kurniawan, F. O. Hidayat, B. H. Aritonang, R. A. Aliyafi, and S. Amri, "A 30-Year Climatological Analysis of Atmospheric Dynamics Anomalies during CENS in Western Indonesia," Journal of Maritime Policy Science, vol. 2, no. 3, pp. 146–157, 2025, doi: 10.31629/jmps.v2i3.7974.

[6] D. Septian, W. S. Zahran, and R. A. Utami, "Analisis Kinerja Anggota Satpol PP Kota Bekasi Dalam Penertiban Pedagang Kaki Lima di Kota Bekasi," Jurnal Ilmu Administrasi Publik, vol. 3, no. 3, pp. 363–370, 2023.

[7] N. H. Saji, B. N. Goswami, P. N. Vinayachandran, and T. Yamagata, "A Dipole Mode in the Tropical Indian Ocean," Nature, vol. 401, pp. 360–363, 1999.

[8] H. Hersbach, B. Bell, P. Berrisford, S. Hirahara, A. Horányi, J. Muñoz-Sabater, J. Nicolas, C. Peubey, R. Radu, D. Schepers, A. Simmons, C. Soci, S. Abdalla, X. Abellan, G. Balsamo, P. Bechtold, G. Biavati, J. Bidlot, M. Bonavita, G. D. Chiara, P. Dahlgren, D. Dee, M. Diamantakis, R. Dragani, J. Flemming, R. Forbes, M. Fuentes, A. Geer, L. Haimberger, S. Healy, R. J. Hogan, E. Hólm, M. Janisková, S. Keeley, P. Laloyaux, P. Lopez, C. Lupu, G. Radnoti, P. D. Rosnay, I. Rozum, F. Vamborg, S. Villaume, and J. Thépaut, "The ERA5 Global Reanalysis," Quarterly Journal of the Royal Meteorological Society, vol. 146, no. 730, pp. 1999–2049, Jul. 2020, doi: 10.1002/qj.3803.

[9] A. Lumbangaol and A. Munandar, "Atmosphere Dynamic Analysis of Hail and Whirl Wind in Cianjur Regency, West Java (Case Study November 07, 2016)," in the 1st International Conference on Science, Mathematics, Environment, and Education (ICoSMEE), ICoSMEE PROCEEDING, 2018, pp. 127–135.

[10] N. H. Muzaki, E. Diniyati, R. R. Pratama, and A. Mulya, "Analisis Kondisi Atmosfer Saat Kejadian Hujan Lebat dan Angin Kencang di Probolinggo Berdasarkan Citra Satelit Dan Citra Radar," JIIF (Jurnal Ilmu dan Inovasi Fisika), vol. 5, no. 2, pp. 142–156, 2021.

[11] A. N. Efendi and S. Kuncorojati, "Analisis Hujan dan Angin Kencang di Melawi Mengunakan Data Radar dan Satelit Cuaca (Studi Kasus Tanggal 29 Desember 2018)," Jurnal Widya Climago, vol. 2, no. 1, 2020.

[12] R. Rafi, D. Kuncoro, B. Arzhida, N. J. Indriyani, and Warjono, "Identifikasi Penyebab Awan Konvektif Pada Fenomena Hujan Ekstrem Disertai Es Berbasis Citra Radar Dual Polar," Jurnal Penelitian Saintek, vol. 3, no. 2, pp. 58–73, 2025, doi: 10.21831/jps.v30i2.89950.

[13] W. Sulistiyono, N. H. S. Salsabil, and S. A. Ramadhan, "Aplikasi Produk Radar C-Band dalam Identifikasi Awan Penghasil Hujan Es (Studi Kasus: Bogor, 24 Januari 2022)," GEOGRAPHIA, vol. 5, no. 2, pp. 137–143, 2024, doi: 10.53682/gjppg.v5i2.8577.

[14] E. I. V. Manurung, S. Humaidi, and Y. Darmawan, "Analysis of Strong Wind Characteristics Using Doppler Weather Radar over Kualanamu Airport Indonesia," JOURNAL OF APPLIED GEOSPATIAL INFORMATION, vol. 8, no. 1, pp. 6–11, 2024.

[15] M. Montopoli, C. Annella, L. Baldini, E. Adirosi, V. Capozzi, and G. Vulpiani, "Rain Motion Vectors Analysis from the Radar Network in Italy," IEEE J. Sel. Top. Appl. Earth Obs. Remote Sens., vol. 17, pp. 11655–11669, 2024, doi: 10.1109/JSTARS.2024.3410031.

[16] H. Adiwira, N. P. Purba, S. A. Harahap, and M. L. Syamsuddin, "Variabilitas Suhu Laut Pada Kejadian IOD (Indian Ocean Dipole) di Perairan Barat Sumatera Menggunakan Data Argo Float," Depik, vol. 7, no. 1, pp. 28–41, Apr. 2018, doi: 10.13170/depik.7.1.8089.

[17] W. J. Pattipeilohy, F. M. B, and D. P. Asri, "Analisis Pengaruh Madden Julian Oscillation (Mjo) Terhadap Anomali Curah Hujan di Wilayah Ngurah Rai," Jurnal Meteorologi Klimatologi dan Geofisika, vol. 6, no. 2, 2019.

[18] J. R. Holton and G. J. Hakim, An Introduction to Dynamic Meteorology, 5th ed. Academic Press, 2013.

[19] M. Sawal, D. A. Siregar, and Y. H. M. Hutabarat, "Analisis Dinamika Atmosfer Kejadian Angin Puting Beliung Tanjung Balai Karimun (Studi Kasus: 14 Mei 2024)," Megasains, vol. 15, no. 2, pp. 38–48, 2024, doi: 10.46824/megasains.v15i2.237.

[20] W. Sulistiyono, R. Surya Ramadhan, and Y. D. Haryanto, "Kajian Kondisi Atmosfer Saat Kejadian Hujan Lebat di Kota Surakarta Menggunakan Analisis Skala Meteorologi (Studi Kasus: 3 Februari 2021)," OPTIKA, vol. 7, no. 1, pp. 32–45, 2023.

[21] N. Kusumawardani and A. A. Azani, "Kajian Indeks Stabilitas Atmosfer Terhadap Kejadian Hujan Lebat Di Kota

Bitung:(Studi Kasus Tahun 2020-2021)," Jurnal Widya Climago, vol. 4, no. 1, 2022.
[22] A. G. Fernanda, A. Ihwan, and R. Adriat, "Analisis Indeks Stabilitas Udara pada Saat Kejadian Angin Puting Beliung di Kota Pontianak," PRISMA FISIKA, vol. 12, no. 01, pp. 6–19, 2024.
[23] D. L. A. Purba, I. J. A. Saragih, and D. S. Sosaidi, "Utilization of weather-radar data to observe the Sea Breeze Front (SBF) over the North Coast of Banten-Jakarta (case study in 2018)," in IOP Conference Series: Earth and Environmental Science, IOP Publishing Ltd, Nov. 2021, pp. 1–14. doi: 10.1088/1755-1315/893/1/012055.
[24] T. M. Smith and K. L. Elmore, "The Use of Radial Velocity Derivative to Diagnose Rotation and Divergence," in 11th Conference on Aviation, Range, and Aerospace Meteorology (ARAM) and 22nd Conference on Severe Local Storms (SLS), American Meteorological Society (AMS), 2004.
[25] M. A. Miller, S. E. Yuter, N. P. Hoban, L. M. Tomkins, and B. A. Colle, "Detecting wave features in Doppler radial velocity radar observations," Atmos. Meas. Tech., vol. 15, no. 6, pp. 1689–1702, Mar. 2022, doi: 10.5194/amt-15-1689-2022.
[26] R. A. Madden and P. R. Julian, "Description of Global-Scale Circulation Cells in the Tropics with a 40-50 Day Period," J. Atmos. Sci., vol. 29, pp. 1109–1123, 1972.
[27] Y. M. Yang and B. Wang, "Improving MJO simulation by enhancing the interaction between boundary layer convergence and lower tropospheric heating," Clim. Dyn., vol. 52, no. 7–8, pp. 4671–4693, Apr. 2019, doi: 10.1007/s00382-018-4407-9.
[28] Selex ES GmbH, "Rainbow® 5 File Format: Phenomena Detection Products," Neuss, Germany, 2016.